Fuzzy Logic Based Delamination Detection in CFRP Panels

Shanglei Li
Dept. of Electrical and Computer Engineering,
Southern Illinois University Carbondale, IL 62901, USA
E-mail: shanglei@siu.edu, http://www.engr.siu.edu/IMEL/

Anish Poudel and Tsuchin Philip Chu
Dept. of Mechanical Engineering and Energy Process,
Southern Illinois University Carbondale, IL 62901, USA

This paper presents an intelligent interpretation of ultrasonic C-scan results for carbon-fiber-reinforced plastic (CFRP) panels by using fuzzy logic approach. Ultrasonic C-scan results have relatively low resolution and poor imaging quality in anisotropic composites due to the speckle noise produced by the interference of backscattered signals. In this study, fuzzy logic was implemented to accurately determine a defect's shape and size and to avoid over-segmentation and under-segmentation. For this, first, a 3×3 mask was considered to define the central value and the mean value within the C-scan amplitude data. Then, five linguistic labels for the central value and mean value were defined as: very low, low, neutral, high, and very high so as to determine fuzzy sets for the fuzzy inference system (FIS). Combined with 25 fuzzy rules, the FIS was capable of making decisions based on fuzzy sets and fuzzy rules. Experimental results demonstrated this fuzzy logic method can detect the size and shape of sub-surface delamination correctly, and restrain the noises effectively. The authors believe this approach for automatic defect detection and classification can be an integral part of the development of an intelligent NDE expert system for composite structures in the future, thus making defect evaluation process much easier and more accurate.

Povzetek: Predstavljena je inteligentna metoda mehke logike za analizo z ogljikom ojačane plastike.

1 Introduction

Carbon-fiber-reinforced plastic (CFRP) panels are now widely being used in many structural applications, especially in the aviation industry, due to their superior thermal and physical properties compared to metals. However, low velocity impacts, for instance, bird or hail strikes on an aircraft, can cause impact damage in CFRP structures. Such damage can take the form of cracking, delaminations, or fiber fractures [1, 2]. The damages in CFRP structures are usually complicated and highly dependent on the properties of the constituent materials, fiber orientation, stacking sequence, and nature of loading [3]. Therefore, a fast and reliable non-destructive evaluation (NDE) process is constantly required to economically ensure the integrity, safety, and reliability of these structures. Ultrasonic NDE is increasingly being used in composite inspection because of its large surface, speed, and non-contact testing capabilities [4-7]. However, due to the anisotropic properties and non-homogeneous behavior of these structures, they have brought a lot of challenges in the NDE industry. One critical problem is how aggressively to decide whether or not variations in the C-scan results are defects [8]. Another problem is the risk of under-segmentation or over-segmentation of the defect area. Both incidents will affect the size, location, and even features of defects, which are critical for defect evaluation. To meet these challenges, various imaging segmentation approaches [9, 10] have been reported to aid the inspection technique. Most segmentation algorithms are based on discontinuity and similarity. In the first category, an abrupt change in density is considered as the edge. Typical edge detection algorithms are Laplacian of a Gaussian (LoG) and Zero crossings. In the second category, segmentation is achieved by partitioning an image into similar density regions according to a set of predefined criteria. Image thresholding and region growing, splitting and merging are typical algorithms in this category. However image segmentation is still one of the most difficult tasks in image processing. Segmentation accuracy determines the eventual success or failure of computerized analysis procedures [10]. A study has demonstrated that rule based algorithms have better performance than the traditional image segmentation method in distinguishing defect areas [11, 12].

For this work, a rule based fuzzy logic approach was applied to solve this problem. The algorithm utilizes the fuzzy inference system of a center element and its eight neighboring elements to define a new objective function and determine the variance by classifying the function. The paper is organized as follows: a discussion of the basic theory, algorithm of fuzzy logic rules, and the experimental setup. They are then followed by the

experimental result. Finally, conclusions are provided at the end.

2 Fuzzy logic theory and application

Fuzzy logic originally developed by Zadeh [13] is not a logic that is fuzzy, but the logic that is used to describe fuzziness. It is an integral component of an expert system and has been widely implemented in many control and prediction systems because it can tackle many problems under various assumptions and approximations with greater accuracy. In addition, its extraordinary controlling and reasoning capabilities have also made it popular in many complex industrial systems. In a fuzzy system, it is possible to define expert knowledge even if statistical data is not available. A fuzzy rule is mathematically described as a fuzzy relation between the sets describing the antecedent and consequent. Each rule in a fuzzy logic is expressed by the following relation [14]:

$$R_i = \left\{ \begin{array}{c} \left((x,y),\mu_R(x,y)\right)| \\ (x,y) \in A_i \times B_i, \mu_R(x,y) \in [1,0] \end{array} \right\} \quad (1)$$

where, $x \in$ X and $y \in$ Y, A_i and B_i are fuzzy subsets of the domains X and Y associated with linguistic labels, $R_i(x,y)$ is a fuzzy relation defined on the Cartesian product universe X × Y.

A general fuzzy inference system (FIS) is shown in Figure 1. It consists of crisp input, fuzzifier, knowledge base, inference methods, deffuzifier, and a crisp output. The FIS takes a crisp input and determines the degree to which they belong to each of the appropriate fuzzy sets via membership functions. A membership function is a curve that defines how each point in the input space is mapped to a membership value. The fuzzifier then measures the value of input variables and performs a scale mapping that transfers the range of values of input variables into corresponding universes of discourse. The knowledge base consists of fuzzy sets and fuzzy rules. Fuzzy sets provide the necessary definitions which are used to define linguistic rules and fuzzy data manipulation, and fuzzy rules characterize the control goals and control policy of domain experts by means of a set of linguistic control rules.
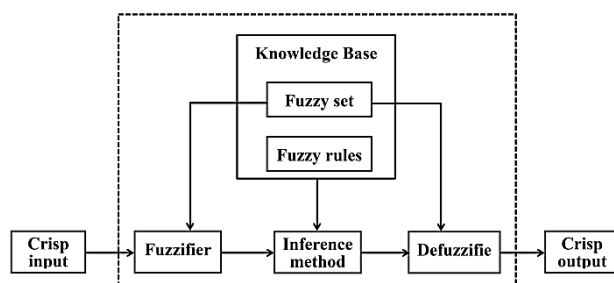

Figure 1: Fuzzy Inference System.

The inference method is the kernel of the FIS and it has the capability of making decisions based on fuzzy sets and fuzzy rules. Finally, defuzzifier performs a scale mapping that converts the range of values of output variables into corresponding universes of discourse.

3 Fuzzy logic algorithm

3.1 Central value and local mean value

The C-scan result obtained from ultrasonic testing is a 2D matrix corresponding to the plan-type view of the location and size of the test specimen. Each element of the matrix indicates the coordinate and the amplitude of received signals. Let $x(i,j)$ be the ultrasonic amplitude data of the element (i,j) in a two dimensional M × N matrix. The mask is defined as a $(2m+1) \times (2n+1)$ window centered at (i,j) where m and n are integers. This window will go through each element to obtain central amplitude and local mean amplitude values of every element in the M × N matrix. Note that the window's shape is not necessarily a square. The central amplitude value is:

$$C_x(i,j) = x(i,j) \quad (2)$$

The local mean of an element (i,j) can be computed as:

$$m_x(i,j) = \frac{1}{(2m+1)\times(2n+1)} \sum_{l=j-n}^{j+n} \sum_{k=i-m}^{i+m} x(k,l) \quad (3)$$

In equations (2) and (3), the parameters of the central value distribution and local mean value distribution for a given matrix are strongly dependent on the window size $(2m+1) \times (2n+1)$. For this, the data are assumed strongly correlated between the central element and its $m \times n - 1$ neighbors. Thus, the computed central amplitude and local mean amplitude will increase as the window size is increased. The window size also depends on the detail pattern as well as the C-scan data "resolution" (step increment of x and y axes). Higher resolution C-scans should use larger window sizes to facilitate the visualization of local details. However, a large window increases the computational requirement. Thus, there is a trade-off between the enhancement of local details and computational loading when determining the proper window size. In this study, to simplify the task, we choose $m = n = 1$, i.e. a 3×3 window as shown in Figure 2. For the given CFRP specimen A, the 2D matrix of C-scan result has 361×961 elements. A 3×3 window is large enough to carry sufficient detail and small enough to keep lower computational time in the whole 2D matrix area.

$i-1,$ $j-1$	$i,$ $j-1$	$i+1,$ $j-1$
$i-1,$ j	i,j	$i+1,$ j
$i-1,$ $j+1$	$i,$ $j+1$	$i+1,$ $j+1$

Figure 2: Applied 3×3 mask with $m = n = 1$.

3.2 Membership functions

The central value and local mean value for a 3 x 3 mask were used to define the membership functions. For this,

five linguistic labels for the central value and the mean value were defined as very low, low, neutral, high, and very high. These levels are based on threshold values for each element amplitude signal value. For example, low amplitude indicates less received ultrasonic signal, which has a greater probability to be classified as a defect. The central value classes are denoted as C_{VL}, C_L, C_N, C_H, and C_{VH}. Similarly, the local mean value is classified as M_{VL}, M_L, M_N, M_H, and M_{VH}. To separate different classes, 4 groups predefined thresholds α_1, β_1 ... ... α_4, β_4 are used as shown in Figure 3. These threshold values are determined experimentally. As an example, if a central amplitude value falls into the range of [β_3, α_4], it will be classified to "High" as C_H. If the value falls into [α_3, β_3], it partially belongs to both "Neural" and "High". In this case, 2 fuzzy rules are fired to determine the output linguistic label of this value. Similar functions and classes are determined for local mean values. Different values fall into different intervals and are classified into the corresponding linguistic labels (classes) appropriately. The linguistic labels and membership functions are depicted in Figure 3.
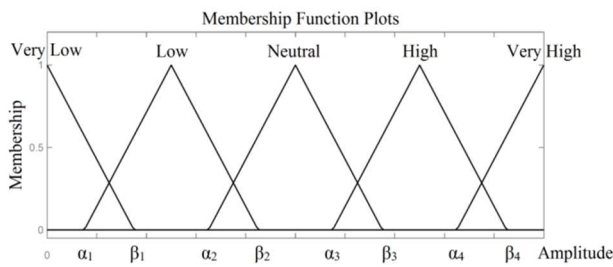

Figure 3: Input variable membership functions and thresholds.

For the output variable, 5 labels were attributed: VL (Very Low) indicating it is a positive defect, L (Low) indicating a potential defect, N (Neutral) indicating it may or may not be a defect, H (High) indicating a potential good area, and VH (Very High) indicating a positive good area. The inference method proposed by Sugeno was utilized in the output which is a constant value for each linguistic label of the variable in the range [0, 1]. The 5 output linguistic labels O_{VL}, O_L, O_N, O_H, and O_{VH} are shown in Figure 4.
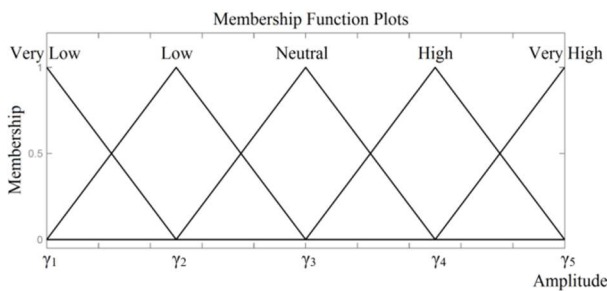

Figure 4: Output variable membership functions and thresholds.

3.3 Fuzzy logic rules

In the fuzzy inference system, fuzzy rules are usually elaborated arbitrarily based on experience and expert decision. It is impractical or impossible to find exact rule sets made by a mathematical formula or model. Especially for sufficiently complex problems, such as defect detection, mathematical methods cannot generate accurate sets of rules. In this case, mathematical methods can only support rules that have already been created. Thus, manual intervention based on expert knowledge is still required. Although most fuzzy rules cannot be accurately developed by a mathematical method, if one of the rules is wrong, even greatly wrong, the fuzzy inference system will compensate for the error just by firing the other correct rules. However, fuzzy rules should be decided carefully by using prior knowledge and NDE expert experience to avoid underperformance in the fuzzy inference system. These rules should be tested vigorously and refined if necessary.

For this study, two variables (central value and local mean value) are utilized as fuzzy inference system inputs; fuzzy logic rules are defined as the following:

Rule Number	Inputs		Outputs (O)	
	Central Value(**C**)	Mean Value(**M**)		
R1	VL	VL	L	Positive defect
R2	VL	L	VL	Positive defect
R3	VL	N	L	Potential defect
R4	VL	H	N	May or not be a defect
R5	VL	VH	H	Potential good area
R6	L	VL	VL	Positive defect
R7	L	L	L	Potential defect
R8	L	N	N	May or not be a defect
R9	L	H	H	Potential good area
R10	L	VH	VH	Positive good area
R11	N	VL	L	Positive defect
R12	N	L	L	Potential defect
R13	N	N	N	May or not be a defect
R14	N	H	H	Potential good area
R15	N	VH	VH	Positive good area
R16	H	VL	L	Potential defect
R17	H	L	N	May or not be a defect
R18	H	N	H	Potential good area

Rule Number	Inputs		Outputs (O)	
	Central Value(**C**)	Mean Value(**M**)		
R19	H	H	H	Potential good area
R20	H	VH	VH	Positive good area
R21	VH	VL	N	May or not be a defect
R22	VH	L	H	Potential good area
R23	VH	N	VH	Positive good area
R24	VH	H	VH	Positive good area
R25	VH	VH	VH	Positive good area

Table 1: Fuzzy logic rules.

In the fuzzy inference system, multiple rules can fire at once. For instance, if a central value falls into the region of $[\alpha_3, \beta_3]$, the overlap part of linguistic labels "Neutral" and "High", both rules will fire. In case the value is more "High" than "Neutral", the "High" rule will generate a stronger response. The fuzzy algorithm will evaluate the result that fired based on fuzzy rules in Table 1, and use an appropriate defuzzification method to generate the output response.

To make the fuzzy rules easy to visualize, a fuzzy associate matrix is depicted in Table 2.

Mean \ Central	VL	L	N	H	VH
VL	VL	VL	L	N	H
L	VL	L	N	H	VH
N	VL	L	N	H	VH
H	L	N	H	H	VH
VH	N	H	VH	VH	VH

Table 2: Fuzzy rules in associative matrix.

As shown in Table 2, more weight is attributed to the mean values than central values. For instance, if the mean value is VH, but the central value is L, the central value is "isolated" by its 8 neighbors. Such a point should be considered as an independent "mutation" point due to the possibility of noise or system error. Therefore, mean values are given more weight than central values to make sure the local defect information in 3×3 window does not contain a misjudged signal mutation caused by noise. Eventually the output result of this point will be VH.

3.4 Defuzzification

For this study, the central of area (COA) defuzzification method [15] was utilized to obtain a crisp output value

from FIS. In the COA method, first the area under the scaled membership functions and within the range of the output variable is calculated. Then, the geometric center of this area is obtained by using the following equation:

$$y_c^* = \frac{\sum_{i=1}^{n} \mu_i \times \gamma_i}{\sum_{i=1}^{n} \mu_i} \tag{4}$$

where: y_c^* is the desired crisp defuzzification value with the COA method.

μ_i is the ith membership degree of input variables.

γ_i is the ith output class center (output variables membership function).

n is the number of elements in a fuzzy set.

The prod method is applied to both of the conjunction evaluation of the rule antecedents and fuzzy rules implication. The aggregation of the rule outputs is carried out by the sum method. Experiment values of input variables are pre-determined with expert knowledge as follows:

Membership functions of central value:
$C_{\alpha_1} = 0.09, C_{\beta_1} = 0.11, C_{\alpha_2} = 0.15, C_{\beta_2} = 0.17, C_{\alpha_3} = 0.19, C_{\beta_3} = 0.21, C_{\alpha_4} = 0.25, C_{\beta_4} = 0.27$

Membership functions of the mean value:
$M_{\alpha_1} = 0.13$, $M_{\beta_1} = 0.15$, $M_{\alpha_2} = 0.17$, $M_{\beta_2} = 0.19$, $M_{\alpha_3} = 0.19, M_{\beta_3} = 0.21, M_{\alpha_4} = 0.22, M_{\beta_4} = 0.23$

Corresponding to Figure 3, output class center γ_i are pre-determined as:
$\gamma_1 = 0, \gamma_2 = 0.25, \gamma_3 = 0.5, \gamma_4 = 0.75$, and $\gamma_5 = 1$

A simple demonstration is given below to briefly explain how the fuzzy logic algorithm works. For one certain element in a 2D matrix of C-scan result, its central amplitude value is 0.105 V and its mean amplitude value (in 3×3 window) is 0.227 V. According to the input membership sets and defined fuzzy rules, during the fuzzy-inference process, 4 fuzzy logic rules are fired in parallel:

Rule 4 $\mu_4 = \mu(C_{VL}) \times \mu(M_H) = 0.125 \times 0.15$
      $= 0.18175 \to \mu_4$ in N $(\gamma_3 = 0.5)$

Rule 5 $\mu_5 = \mu(C_{VL}) \times \mu(M_{VH}) = 0.125 \times 0.35$
      $= 0.04375 \to \mu_5$ in H $(\gamma_4 = 0.75)$

Rule 9 $\mu_9 = \mu(C_L) \times \mu(M_H) = 0.375 \times 0.15$
      $= 0.05625 \to \mu_9$ in H $(\gamma_4 = 0.75)$

Rule 10 $\mu_{10} = \mu(C_L) \times \mu(M_{VH}) = 0.375 \times 0.35$
      $= 0.13125 \to \mu_{10}$ in VH $(\gamma_5 = 1)$

Based on equation (4), the fuzzy output y^* with COA method can be obtained:

$$y_c^* = \frac{\sum_{i=1}^{n} \mu_i \times \gamma_i}{\sum_{i=1}^{n} \mu_i}$$
$$= (0.18175 \times 0.5 + 0.04375 \times 0.75 + 0.05625$$
$$\times 0.7 + 0.13125 \times 1)/(0.5 + 0.75 + 0.75 + 1)$$
$$= 0.8625 \tag{5}$$

The fuzzy logic output y^* of C-scan data will be normalized to 0~255 and plot in 2D matrix corresponding to column and index, shown as a gray-level image.

4 Experimental setup

The immersion ultrasonic system with associated instrumentation used to inspect the CFRP panel is shown in Figure 5. A 5 MHz dual element Panametric transducer with a 2 inch focal length was utilized in a pulse-echo mode for the inspection. The standoff distance between the transducer and the panel was set to 2 inches and the scan was conducted at an increment of 0.01 inches.
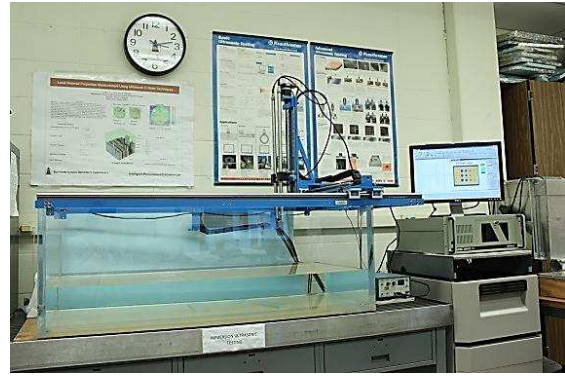

Figure 5: Immersion ultrasonic testing system.

(a) Optical image of specimen A

(b) Optical image of specimen B

(c) Defect map of specimen A
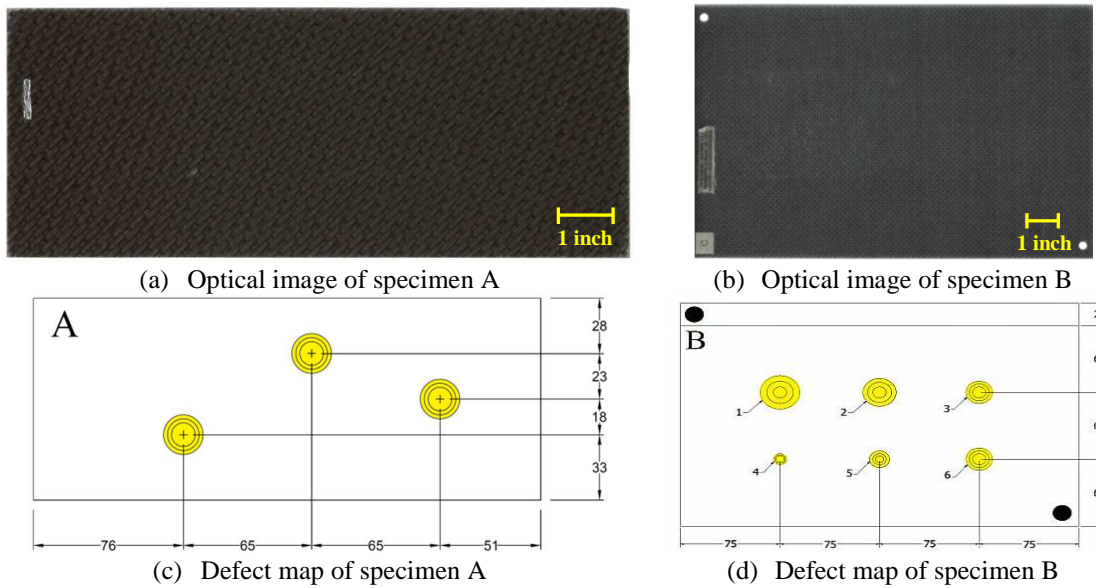

(d) Defect map of specimen B

Figure 6: Optical images and defect maps of specimen A and B. All dimensions are in mm.

To verify the application of fuzzy logic defect detection, two different CFRP panels with predefined phantom defects, i.e. delamination defects due to impact damage were considered. These delamination defects were artificially simulated by impacting the panel with an external object of known energy. These defects are difficult to recognize by visual inspection, but have severely progressed within the panel. Specimen A is a $102 \times 257 \times 4.445$ mm panel which consists of impact damage at three different locations. Similarly, specimen B measured $200 \times 300 \times 3.581$ mm in dimensions. The optical images and defect maps of each specimen are shown in Figure 6.

5 Result and discussion

The fuzzy logic algorithm as described earlier, was applied to the ultrasonic C-scan results (maximum back wall amplitude data) obtained from both panels to verify the versatility and stability of the fuzzy inference system. The proposed method was implemented in MATLAB R2012b. The reconstructed raw C-scan results are presented in Figure7, where defect areas are represented by dark shade of gray i.e. significant drop in pulse-echo signal amplitude. The shaded area labeled "Marker" in Figure 7 is the marker that was attached to the panel for indication purposes.

(a) Reconstructed C-scan image of specimen A

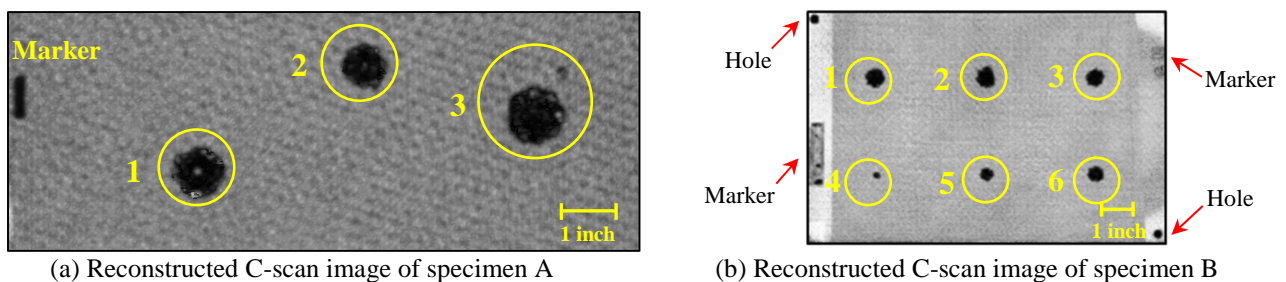(b) Reconstructed C-scan image of specimen B

Figure 7: Reconstructed C-scan result for CFRP panels.

The fuzzy logic output of ultrasonic C-scan data for CFRP panels A and B are normalized and plotted in 8 bit grayscale images (256 gray-level) as shown in Figure 8. Figure 8 (a) and (b) are the fuzzy logic output results with the COA defuzzification method. From the results obtained, the fuzzy logic method is able to detect the

defects with more confidence by eliminating the background compared to the raw C-scan image as in Figure 7 (a) and (b). The defect outline present is more distinct to recognize, allowing post-processing work such as measurement of defect size, shape, and location to be much easier.
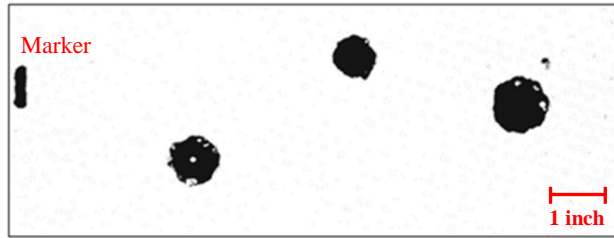
(a) Specimen A fuzzy logic output result image with the COA defuzzification method
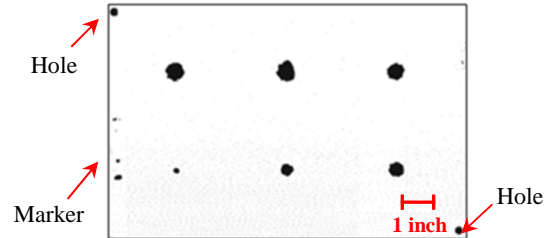
(b) Specimen B fuzzy logic output results image with the COA defuzzification method

Figure 8: Fuzzy logic output results.

To demonstrate the effectiveness and robustness of the fuzzy logic method applied, defects in specimen A and 3 of 6 defects in specimen B are shown in Figure 9 and Figure 10, respectively. The experiment results indicate that the fuzzy logic method has satisfied performance on both CFRP panels (sample A and B), which have different carbon fiber orientation and laminates. As shown in Figure 9 and Figure 10, fuzzy logic results provide a clear and smooth edge area for all defects in sample A and B. The fuzzy logic method is able to remove the background noise in C-scan images to obtain high contrast and enhanced images.
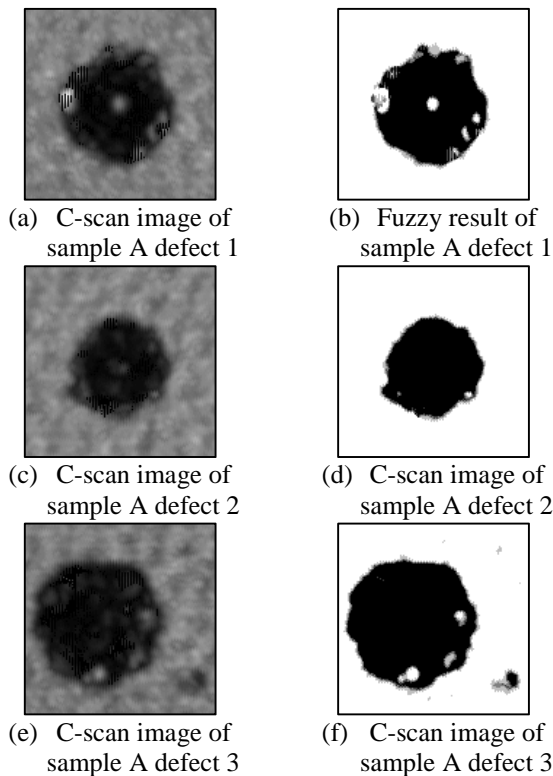

(a) C-scan image of sample B defect 1

(b) C-scan image of sample B defect 1

(c) C-scan image of sample B defect 2

(d) C-scan image of sample B defect 2

(e) C-scan image of sample B defect 3

(f) C-scan image of sample B defect 3

Figure 10: Comparison of C-scan images and fuzzy logic results of 3 defects in specimen B.

(a) C-scan image of sample A defect 1

(b) Fuzzy result of sample A defect 1

(c) C-scan image of sample A defect 2

(d) C-scan image of sample A defect 2

(e) C-scan image of sample A defect 3
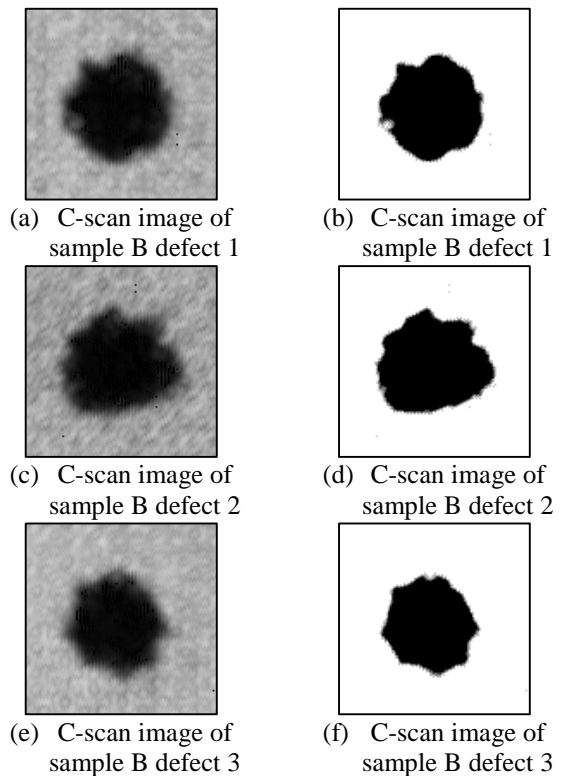
(f) C-scan image of sample A defect 3

Figure 9: Comparison of C-scan images and fuzzy logic results of 3 defects in specimen A.

For subjective evaluation, fuzzy logic output results are compared to the reconstructed C-scan images side by side in Figure 9 and Figure 10. From the results obtained, the fuzzy logic method is able to detect the defects with more confidence by eliminating the noises seen in the C-scan images on the left side. The fuzzy logic output is capable of providing higher contrast of the defect area which allows NDE inspector make accurate decisions to identify the defect size and location.

In addition to the perceived image quality with human visual system (HVS), for objective evaluation, peak signal-to-noise ratio (PSNR) and contrast signal-to-

noise ratio (CNR) are employed for quantitative assessment. The fuzzy logic result and C-scan result are tested to demonstrate the image quality and robustness of the fuzzy logic method,
The PSNR is given as:

$$PSNR = 10 \cdot \log_{10} \left(\frac{MAX_I^{\,2}}{MSE} \right) \qquad (6)$$

Where: MAX_I is the maximum possible pixel value of the image. In this study, all pixels are represented using 8 bits gray levels, here MAX_I is 255.

MSE is the mean squared error between two compared images.

The CNR is given as:

$$CNR = \frac{S_i - S_o}{\sqrt{\sigma_i^2 + \sigma_o^2}} \qquad (7)$$

Where: S_i and S_o are the mean values inside and outside the ROI respectively

σ_i and σ_o are the standard deviations, respectively

	ROI		CNR (dB)	PSNR (dB)
Sample A	Whole Sample	C-scan result	5.63	
		Fuzzy logic	8.97	6.17
	Defect 1	C-scan result	5.09	
		Fuzzy logic	6.20	7.18
	Defect 2	C-scan result	4.38	
		Fuzzy logic	5.07	7.08
	Defect 3	C-scan result	3.83	
		Fuzzy logic	4.69	7.47
Sample B	Whole Sample	C-scan result	3.88	
		Fuzzy logic	5.38	10.06
	Defect 1	C-scan result	3.15	
		Fuzzy logic	4.37	10.20
	Defect 2	C-scan result	3.79	
		Fuzzy logic	4.74	9.32
	Defect 3	C-scan result	2.11	
		Fuzzy logic	2.95	10.34

Table 3: Experimental comparison of CNR & PSNR.

From Table 3, it can be verified that the CNR of the fuzzy logic output is higher than C-scan result. The PSNR has the close value in sample A and B, indicating the quality of the fuzzy logic method is robust and reliable. Further, note that the PSNR value of fuzzy logic output has an average increase of 6.98 dB in sample A and 9.98 dB in sample B compared to C-scan results. Since the applied method provides good performance in both CNR and PSNR, it can be seen that the proposed super-resolution reconstruction method is effective in resolution enhancement.

6 Conclusions

Analysis of the raw C-scan result of composites may not provide the reliable classification of different regions (defect, non-defect). A fuzzy logic methodology is applied to classify the defect and non-defect areas in CFRP panels with simulated delamination defects. The experimental results obtained for these panels have demonstrated the effectiveness of the applied method. It can be used as preprocessing of defect segmentation to reduce the computation complexity and time. However, membership function and fuzzy rules need to be adjusted for different types of CFRP materials to achieve better performance. An automated classification of defect and non-defect areas in composites remains a challenging job which requires a considerable amount of research work to be carried out in future. In addition, the performance of the system can also be improved by studying the correlation between the damage mechanism and the data distribution, and by applying more sophisticated algorithms. Further, better performance can be achieved by constantly updating the knowledge and rules so that the systems can adapt to new kinds of problems.

References

[1] Sihn, S., R.Y. Kim, K. Kawabe, S.W. Tsai, "Experimental studies of thin-ply laminated composites," *Composites Science and Technology*, 64 (6) 996-1008, 2007.

[2] Graham, D., P. Maasa, G.B. Donaldsona and C. Carr. "Impact damage detection in carbon fiber composites using HTS SQUIDs and neural networks," *NDT&E International* 37, 565-570, 2004.

[3] Chu, T.C., A. Leyte, A. DiGregorio, S. Russell and J.L. Walker. "Micro-Cracking Detection in Laminated Composites," *Proc. of ASNT Spring Conference and 11th Annual Research Symposium*, Portland, OR, 2002.

[4] Im, K. H., D.K. Hsu, I. Y. Yang, "Inspection of Inhomogeneities in Carbon/Phenolic Matrix Composite Materials Using NDE Techniques." *Key Engineering Materials*. Vols. 270 – 273, pp 1799-1805, 2004 .

[5] Lee, J.H., S.W. Choi, K.S. Kim, J.H. Park, J.H. Byun, "Nondestructive Characterisation of Carbon/Carbon Brake Disks Using Ultrasonics", http://www.ndt.net/article/apcndt01/papers/1109/1109.htm, 2001.

[6] Ruosi, A., "Nondestructive detection of damage in carbon fiber composite," *Journal of Physical stat.*, Vol, 2(5), pp 1153-1155, March 2005.

[7]   Bray, D.E., McBride, D, *Nondestructive testing techniques*, Wiley-Interscience Publication, John Wiley & Sons, Inc., NewYork, 1992.

[8]   Liu N., Q.M. Zhu, C.Y. Wei, N.D. Dykes, Irving PE. "Impact damage detection in carbon fiber composites using neural network and acoustic emission." *Key Eng Mater*,167-168: 45-54, 1999.

[9]   Zennouhi, R., Lh. Masmoudi, "IEEE - Image segmentation using hierarchical analysis of 2D-histograms - Application to medical images." *Proc. of Multimedia Computing and Systems International Conference*, (s): pp 480- 483, Ouarzazate, 2009.

[10] Gonzalez, R.C. and Woods, R.E. *Digital Image Processing*, 3rd ed., Prentice Hall, Upper Saddle River, NJ, 2008.

[11] Poudel, A., S. Li, T.C. Chu, D. Palmer, and R. Engelbart, "An Intelligent Systems Approach for Detecting Delamination Defects due to Impact Damage in CFRP Panel by Using Ultrasonic Testing", *Proc. of ASNT Fall Conference and 21st Annual Research Symposium*, Palm spring, CA, Oct 2011.

[12] Poudel, A., S. Li, T.C. Chu, D. Palmer, and R. Engelbart, "Neural-Fuzzy Approach in Detecting and Classifying Foreign Object Inclusions in CFRP Panel by Using Ultrasonic Testing", *Proc. of ASNT Fall Conference and 21st Annual Research Symposium*, Palm spring, CA, Oct 2011.

[13] Zadeh, L.A., Fuzzy sets. *Information and Control*, 8, pp. 338-353, 1965.

[14] Negnevitsky, M., *Artificial Intelligence*, Harlow, England: Addison-Wesley, 2005.

[15] Yen, J, and Laungari, R., *Fuzzy logic intelligence, control and information*, Prentice-Hall, Inc., New Jersy, USA, 1999.